

# Energy & Environmental Science

Accepted Manuscript



This is an *Accepted Manuscript*, which has been through the Royal Society of Chemistry peer review process and has been accepted for publication.

*Accepted Manuscripts* are published online shortly after acceptance, before technical editing, formatting and proof reading. Using this free service, authors can make their results available to the community, in citable form, before we publish the edited article. We will replace this *Accepted Manuscript* with the edited and formatted *Advance Article* as soon as it is available.

You can find more information about *Accepted Manuscripts* in the [Information for Authors](#).

Please note that technical editing may introduce minor changes to the text and/or graphics, which may alter content. The journal's standard [Terms & Conditions](#) and the [Ethical guidelines](#) still apply. In no event shall the Royal Society of Chemistry be held responsible for any errors or omissions in this *Accepted Manuscript* or any consequences arising from the use of any information it contains.

## ARTICLE

## Bioelectrodes modified with Chitosan for long-term Energy Supply from the Body

Cite this: DOI: 10.1039/x0xx00000x

S. El Ichi,<sup>a</sup> A. Zebda<sup>a</sup>, J.-P. Alcaraz<sup>a</sup>, A. Laaroussi<sup>b</sup>, F. Boucher<sup>a</sup>, J. Boutonnat<sup>c</sup>, N. Reverdy-Bruas<sup>b</sup>, D. Chaussy<sup>b</sup>, M.N. Belgacem<sup>b</sup>, P. Cinquin<sup>a</sup> and D.K. Martin<sup>a,\*</sup>

Received 00th January 2012,  
Accepted 00th January 2012

DOI: 10.1039/x0xx00000x

www.rsc.org/

The 3D nanofibrous network of compressed chitosan in the presence of genipin as cross-linker, carbon nanotubes and laccase constitutes a new design to enhance the stability and the biocompatibility of biocathodes. The *in vitro* delivered current was around  $-0.3 \text{ mA mL}^{-1}$  during 20 days under continuous discharge. A thin film made of chitosan cross-linked with genipin was synthesized and optimized for oxygen and glucose diffusion. This film was used as a biocompatible barrier on the surface of biocathodes implanted in rats. The biocathodes remained operational after 167 days *in vivo*. This biocathode design minimised the inflammatory response in the first two weeks after implantation. After several months, the growth of macrophages was observed. The electrical connection and the catalytic activity of the enzyme entrapped into the biocathode was demonstrated after almost 6 months of implantation by the *ex vivo* measurement of the OCP (0.45V to 0.48V) and the delivered current ( $-0.6 \text{ mA mL}^{-1}$ ) under optimal conditions.

### Broader Context

The next generation of implantable medical devices require sustainable ways to provide their energy. For an implanted energy supply, sustainability means that the device needs to be compatible with the environment inside the body, the device should not cause any inflammation and the device should be able to utilise biomolecules inside the body as fuel to produce energy. Also, importantly, the implanted power supply should have a very long life-time to continue to produce energy inside the body for other implanted medical devices. In this article we describe a 3D bioelectrode that continued to produce energy electrochemically for around 6 months when implanted inside a freely moving animal. This advance is based on improving the biocompatibility with an innovative design and use of biomaterials. Providing energy for such a long period of implantation, especially in a freely moving animal, is a novel result that addresses the existing issues in this field for the future of implantable energy supplies, namely that is necessary to improve their stability and efficiency. Our results augur well for continuing improvements in the implanted lifetimes of biofuel cells, so as to enable these implantable biofuel cells to become viable and sustainable energy supplies for medical devices.

### 1. Introduction

The search to provide stable and long-lasting power supplies for implanted medical devices has turned to seek novel ways to utilize biomolecules, which are available in the extracellular fluid, as the fuel for biofuel cells. A Glucose Biofuel Cell (GBFC) provides a promising solution for that search because it utilizes enzymes to oxidize glucose and reduce dioxygen in order to generate electrical power. Both glucose and oxygen are freely available in the extracellular fluid, theoretically allowing such a biofuel cell to function indefinitely by relying on the advantageous aspects of enzymatic catalysis which can occur at body temperature and neutral pH. The longevity of such a GBFC relies upon incorporating appropriately stable enzymes in sufficient quantities in bioelectrodes, which would potentially allow this system to provide a more

biologically compatible replacement for the traditional electrocatalysis reactions of conventional fuel cells that are used currently to power medical devices.

To obtain the biomolecules requires controlled exchanges between the implanted GBFC and body fluids. Recently, several teams have reported systems that achieve such exchanges to produce useful levels of electrical energy inside the body. Cinquin and coworkers<sup>1</sup> implanted a GBFC in retroperitoneal space of freely moving rats. The implanted GBFC was based on composite graphite discs containing glucose oxidase and ubiquinone at the anode, polyphenol oxidase (PPO) and quinone at the cathode. They demonstrated that an implanted GBFC was able to produce  $10 \mu\text{W}$  using extracellular glucose and dioxygen. The GBFC was also able to power a light-emitting diode (LED) and a digital thermometer<sup>2</sup>. Sales and

coworkers<sup>3</sup> developed an implantable glucose/dioxygen hybrid enzyme–Pt micro-biofuel cell, and demonstrated that this GBFC implanted in the jugular vein of a rat was capable to produce 200  $\mu\text{W cm}^{-2}$ . Katz and coworkers demonstrated that GBFCs connected in series or in parallel deliver enough power to supply an electric motor<sup>4</sup> and a cardiac pacemaker<sup>5</sup>. Andoralov and coworkers<sup>6</sup> succeeded to produce 2  $\mu\text{W cm}^{-2}$  using a GBFC implanted in cerebrospinal fluid and in the brain of a rat.

Those results constitute a considerable advance in the development of implantable glucose biofuels. Nonetheless, the major challenge with any of those GBFCs continues to be short life-time, poor stability and poor biocompatibility during implantation so that GBFCs published to date have been unable to supply power continuously for long periods of time when implanted. Biofouling of the semi-permeable membranes, filtration capacities and general biocompatibility issues of the materials used for the bioelectrodes remain hurdles that diminish the power output, for even short-term implantation.

The bioelectrodes necessary for the power output from a GBFC include a bioanode to oxidize glucose and a biocathode to reduce dioxygen. The existing research indicates that either glucose oxidase (GOD) or glucose dehydrogenase is an appropriate enzyme for the bioanode and that laccase or bilirubin oxidase (BOD) is an appropriate enzyme for the biocathode<sup>7,8</sup>. When implanted, some components of the extracellular fluids affect GBFC function, particularly in the case of the biocathode. Indeed, BOD activity is irreversibly and rapidly damaged by urate in the presence of dioxygen<sup>7</sup>, and laccase activity is affected by the high concentration of chloride anions<sup>8</sup>. However, some authors observed that in the case of direct electron transfer (DET) between laccase and the electrode, without any chemical mediator, laccase preserves its activity<sup>9–11</sup>. This resistance to chloride was attributed to the fact that chloride is a competitive inhibitor of laccase<sup>9</sup>. In the case of a compressed laccase-carbon nanotube (MWCNT) pellet, laccase remains active for several weeks at neutral pH<sup>10,11</sup>. However, the activity of laccase decreases substantially at physiological pH, since laccase has an acidic optimal pH. To solve this problem, it was proposed to use at the cathode the enzyme PPO which is capable to work in physiological serum without any inhibition<sup>1</sup>. The disadvantage of PPO is its low redox potential 250 mV *vs.* Ag/AgCl, which is 150 mV lower than that of BOD and half the redox potential of laccase.

Recently, we have developed means to improve the stability of the biocathode. We demonstrated that the encapsulation of laccase in a composite of Chit-MWCNT fibres provides the capability for the biocathode to work in physiological pH, for two months in a continuous mode, and stable for several months when stored at neutral pH and periodically tested<sup>12</sup>. Chitosan is a natural semi-crystalline polysaccharide derived from chitin, which is the second most abundant biopolymer after cellulose. It can be extracted from different sources (crustacean shells, insect cuticles, mushrooms envelopes, green algae cell walls, and yeasts)<sup>13,14</sup>. Chitosan is biocompatible and especially useful for many applications in the biomedical field<sup>15,16,17</sup>. The ratio of D-glucosamine to the sum of D-glucosamine and N-acetyl D-glucosamine gives the number of amino groups along the chains, which then determines the deacetylation degree of chitosan. The degree of deacetylation is important, since the amino groups can react with different molecules such as proteins<sup>18</sup> and cross-linkers (glutaraldehyde, etc.).

In this paper, we report the novel use of chitosan crosslinked with genipin to enhance the stability and the biocompatibility of the biocathode when implanted for long periods in an animal. Genipin is

obtained from geniposide which is isolated from the fruits of *Gardenia jasminoides* Ellis. It is very attractive for improving the performance of the biocathode, since it is a natural crosslinker which reacts with amine groups of polymers and it is 10,000 times less toxic than glutaraldehyde<sup>19,20</sup>. Moreover, genipin is an anti-inflammatory and anti-angiogenesis agent.

## 2. Experimental section

### 2.1. Enzyme and chemical

Laccase from *Trametes versicolor*, high viscosity chitosan were purchased from Sigma-Aldrich (Saint Quentin Fallavier, France). Phosphate Buffer Saline (PBS) tablets (0.01 mole L<sup>-1</sup>, 0.14 mole L<sup>-1</sup> NaCl, 0.0027 mole L<sup>-1</sup> KCl, pH 7.4) were purchased from Euromedex (Souffelweyersheim, France). Silicone (AS310) was purchased from SILICOMET. All aqueous solutions were prepared using ultrapure water from Millipore system. Multi-walled carbon nanotubes (MWCNTs) were purchased from Nanocyl (> 95 % purity, 9.5 nm diameter). The Dacron vascular graft was supplied by P. Porcu, Service de chirurgie vasculaire, CHU Grenoble. The Wistar Han IGS male rats were purchased from Charles River.

### 2.2. Chitosan film synthesis

Viscous chitosan (1 % (m/v) solubilized in 0.5 % (v/v) acetic acid at 50°C) was obtained after 2 hours stirring at ambient temperature. A genipin solution (6 mg mL<sup>-1</sup>) was prepared by solubilizing the genipin powder in 12 % (v/v) DMSO, 88 % (v/v) H<sub>2</sub>O. A volume of 150  $\mu\text{L}$  of this solution was added to the 20 mL chitosan. The final concentration of genipin is 4.5 % (m/v) in 1 % (m/v) chitosan. The mixture was stirred for 30 min.

For the film casting, a volume of about 3 g of viscous chitosan was deposited on a non-adhesive circular surface (28 cm<sup>2</sup>). For this purpose, a ROTH-disposable weighing tray (PS natural coloured L 89 × W 89 × H 25 mm) was used. Then, it was dried at ambient temperature for a minimum of 72 hours to obtain a dry plastic film.

### 2.3. Thickness measurement

The thickness of the chitosan plastic membranes was measured using a digimatic indicator (0.0001-1.2") from Mitutoyo (Roissy CDG, France). The device was used to measure the thickness at 10 locations, chosen at random, across the surface of the membrane. The value of thickness for the membrane was reported as the mean of 10 measurements.

### 2.4. FTIR analysis

Fourier Transformed Infrared (FTIR) spectra of chitosan films were obtained using a PERKIN ELMER PARAGON 1000 spectrometer. A total of 16 scans were performed at 4 cm<sup>-1</sup> resolution. Measurements were recorded between 4000 and 600 cm<sup>-1</sup>. Each FTIR spectrum was obtained in transmittance mode.

### 2.5. Atomic force microscopy (AFM)

In order to determine the surface roughness of chitosan films, AFM experiments in a tapping mode were conducted on an SPI 3800N probe station (Seiko Instruments Inc., Japan). A resonance frequency of 10 kHz was used for all experiments with a 1  $\mu\text{m}$  scanner. All AFM experiments were performed in air.

### 2.6. Biocathodes preparation

The viscous chitosan-genipin solution was prepared as described previously. For the fabrication of the biocathode that included chitosan, a mixture of laccase from *Trametes versicolor* (100 mg), MWCNTs (100 mg) and viscous chitosan-genipin (200  $\mu$ L) was used. The resulting mixture was divided into 5 equal quantities in order to prepare 5 disks compacted using a manual press. In order to perform the electrical connection, a wire was embedded in carbon paste covering one side of each disk (surface: 0.5 cm<sup>2</sup>, thickness: 1 mm). The perimeter and the covered side of the disc were isolated with silicone. The cathodes were dried at ambient temperature and then stored at 4 °C until use.

### 2.7. Scanning electronic microscopy (SEM)

The structure of the film and the biocathodes before and after implantation in rats was characterized by SEM using an ULTRA 55 FESEM based on the GEMINI FESEM column (Nanotechnology Systems Division, Carl Zeiss NTS GmbH). Samples were sputter-coated with 1 nm gold-palladium using precision etching coating system (PECS 682- Gatan, Inc., CA).

### 2.8. Sterilisation by gamma radiations

The irradiator uses sources of <sup>60</sup>Co (ARC-nucleart CEA grenoble). Three gamma doses were tested for the sample irradiation: 6, 12 and 42 kGy. The effect of the gamma radiation on the free and immobilized enzyme in the cathodes was studied and compared to non-irradiated samples before the determination of the adequate gamma dose for sterilization (12 kGy).

### 2.9. Implantation of bioelectrodes in the body of rats

Four rats were used for the *in vivo* study, which was approved by the Committee on the Ethics of Animal Experiments of the Grenoble University (ComEth, number: 243 LER-UMR7525-JPA-01). The care of the rats was approved by the European Communities Council Directive Animal Care and Use Committee, and the experiments performed in accordance to their guiding principles (European Communities Council Directive L358-86/609/EEC) and also under license from the French Ministry of Agriculture (numbers 38018 and 381141).

Four implants were prepared (one biocathode for each rat). Two implants have been used for the histological characterization while the two others were used for the electrochemical tests. The copper wire connected to the biocathode was isolated with a catheter. The biocathode was enclosed within a Dacron bag (Fig. 1) and sterilized by gamma radiations, as described above. The rat was anesthetized, a median laparotomy performed, and the cathode inserted into the retroperitoneal space in left lateral position. The muscular abdominal wall and the skin were separately sutured and the animal allowed to recover from anesthesia.

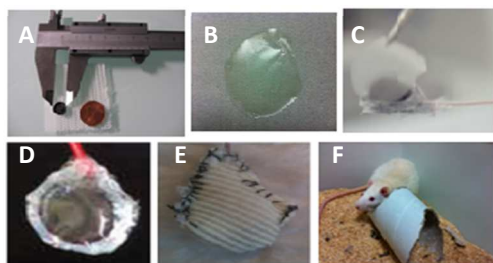


Figure 1: (A) Chit-MWCNT-laccase electrode, (B) Plastic chitosan-based film, (C) Film coating of the surface of the electrode, (D) Chit-MWCNT-laccase electrode coated with the chitosan film,

(E) implantable electrode inside a Dacron bag, (F) Rat with implanted biocathode

For the period post-operatively up to 167 days the rats were fed with a standard diet and water ad libitum in a room with a 12h light/dark cycle at a temperature of 22 $\pm$ 2°C. The weight and food consumption of the rats was measured regularly. The rats gained weight during the post-operative period, from the average weight of 457 $\pm$ 41 g at the first post-operative day, to an average weight of 531 $\pm$ 34 g after 90 days. After the 167 the weight of the rat was 572 g. The rats maintained their consumption of food during the period of implantation, at 21 $\pm$ 8 g (first post-operative day) to 24 $\pm$ 3 g (after 90 days) and 26 g (after 167 days).

After the period of implantation, two biocathodes were analyzed *ex vivo*. The implant (Fig. 7A) was removed. The Dacron bag covered with growing tissues was opened carefully (Fig. 7C) to take out the biocathode which was immersed in PBS pH 7.4 and analyzed in the electrochemical cell as described in section 2.11.

### 2.10. Histological characterization of implanted biocathodes

Immediately after their extraction from the rat body, the samples were immersed for 24 h in 4 % formaldehyde solution. The processing of cassettes containing those tissue samples was performed automatically in a Semi-Enclosed Benchtop Tissue Processor Leica TP1020. The embedding in paraffin was carried out using a Heated Paraffin Embedding Module Leica EG1150 H. The sectioning into 4  $\mu$ m slices was carried out using a Semi-Automated Rotary Microtome Leica RM2245. A routine trichromic HES (Hematoxylin-Eosin-Safran) histological stain was performed. In the images of the histological slices (Fig. 8), the purple color in the presence of hematoxylin corresponds to the nuclei, eosin stains the cytoplasm in pink and collagen fibers are colored orange by safran. Microscopic observation was done under the Zeiss microscope (SAMBATM 2050) at different magnifications (X10, X20 and X40).

### 2.11. Electrochemical assays

All electrochemical measurements were performed using an electrochemical potentiostat (Biologic, 300). Measurements were performed using a conventional three-electrode cell (80 cm<sup>3</sup>). The biocathode was analyzed in 100 mL of a phosphate buffer saline pH 7.4. A saturated calomel electrode (SCE) was used as reference electrode and a platinum mesh as a counter electrode. The chronoamperometric response of the biocathode was recorded at 0.2 V vs. SCE. In the same conditions, cyclic voltammetry at different scan rates (0.2, 0.3, 0.4, 0.5, 0.6, 0.7 mV s<sup>-1</sup>) was performed to monitor the current in response to variations in potential. All measurements were performed at ambient temperature (20  $\pm$  3 °C).

## 3. Results and discussion

### 3.1. Characterization of the chitosan film

As shown in Fig. 1, the chitosan film cross-linked with genipin is bluish green. This colour is due to the reaction between genipin and the amino groups of the chitosan, which is expected to produce a dark blue colour<sup>21</sup>, but in our case the lighter color indicates low genipin content. The chitosan-genipin cross-linking reaction involves several stages<sup>22</sup>. An oxygen-radical induced polymerisation of genipin occurs after formation of an heterocyclic compound during reaction steps. The resultant chitosan-genipin polymer is insoluble in acidic and alkaline conditions and its swelling properties depend on pH and temperature<sup>22</sup>.

An FTIR-ATR analysis of uncross-linked and genipin-cross-linked chitosan films was carried out in order to study the chemical changes of chitosan after cross-linking (Fig. 2A).

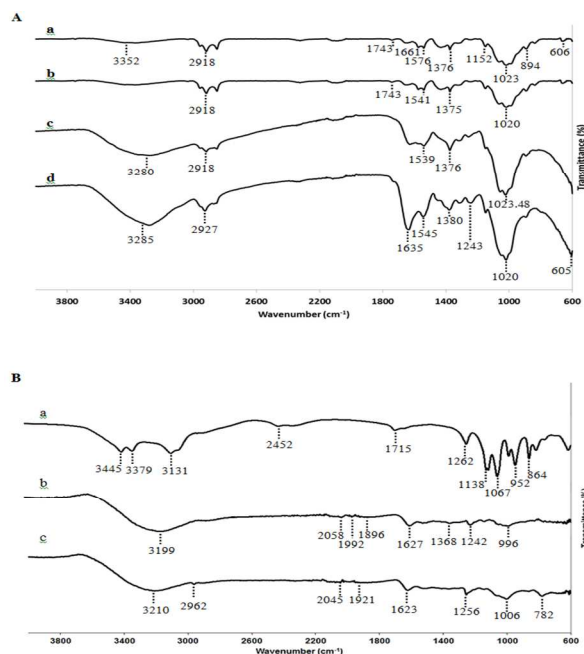


Figure 2: FTIR analysis of (A) the chitosan films: (a) chitosan, (b) chitosan cross-linked with genipin, (c) after 90 days *in vivo*, (d) after 167 days *in vivo*, (B) Chit-MWCNT-laccase biocathode: (a) stored *in vitro*, (b) after 90 days *in vivo*, (c) after 167 days *in vivo*.

Chitosan (curve (a)) presents OH stretching band at  $3352\text{ cm}^{-1}$ , C-H stretching peak at  $2918\text{ cm}^{-1}$ , C-O-C stretching signal at  $1023\text{ cm}^{-1}$ , C-O-C bridges and glycosidic linkages at  $894\text{ cm}^{-1}$ . This is in accordance with IR characteristic bands of chitosan found in the literature<sup>23,24</sup>. The peak at  $1376\text{ cm}^{-1}$  (curve (a)) is assigned to the methyl groups ( $-\text{CH}_3$ ) symmetric deformation. This peak is broader in the other three curves which correspond to the presence of ring-stretching of heterocyclic amine after cross-linking with genipin<sup>25</sup>.

In curve (a), the absorption peak at  $1661\text{ cm}^{-1}$  (C-O stretching) and  $1576\text{ cm}^{-1}$  (N-H stretching) corresponds to the amide I band. The peak observed at  $1576\text{ cm}^{-1}$  is assigned to the vibrational band corresponding to primary amino groups after N-acetylation of chitosan. This is characteristic of chitosan with high deacetylation degree<sup>26</sup>. The amide I band shifted to  $1541\text{ cm}^{-1}$  (curve (b)) after genipin cross-linking. This band is retrieved at  $1539\text{ cm}^{-1}$  (curve (c)) and  $1545\text{ cm}^{-1}$  (curve (d)). The cross-linking mechanism consists of the reaction of amino groups of chitosan with genipin which results in amide linkage and heterocyclic amine. Due to the overlapping of the C=O stretching band of chitosan with the C=C stretching in cyclic structure of genipin, the amide I band became slightly broader in curve (b) and this is intensified in curve (c) and (d). This intensification can be due to the reaction of free amino groups with other proteins present in the extracellular fluid. A broad peak at  $1635\text{ cm}^{-1}$  and  $1243\text{ cm}^{-1}$  (C-N stretching of amide III) were noticed in curve (d) which indicates that new cross-linking reactions have indeed occurred *in vivo*. The peak at  $1743\text{ cm}^{-1}$  corresponds to the carboxylic groups of chitosan.

Fig. 3C and D show the dry chitosan film. Fig. 3E and F show SEM images corresponding to the structure of the wet chitosan film after swelling in the buffer solution. The dry film shows a stratified structure which disappeared after swelling. The difference between

the thickness of the dry and wet film doesn't exceed a few nanometres.

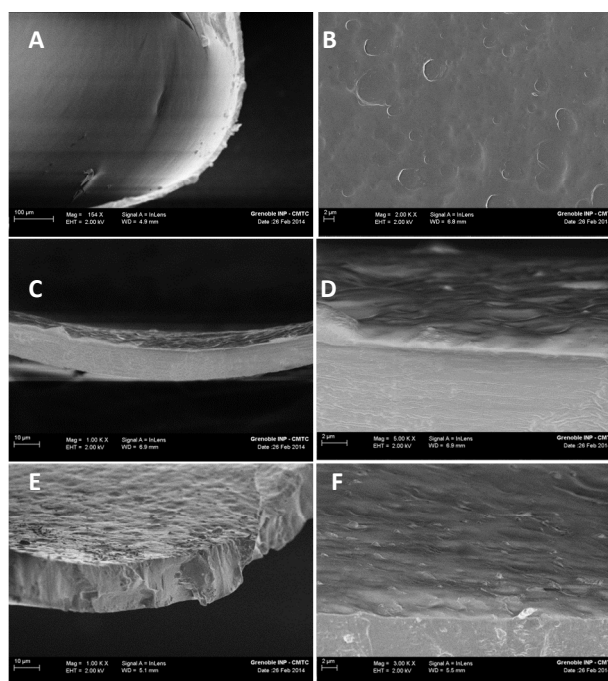


Figure 3: SEM images of (A) Smooth and (B) rough side of the dry film, (C) cross-section and (D) rough surface of the dry film, (E) cross-section and (F) surface of the hydrated film

The mean thickness of the chitosan film is about  $15\text{ }\mu\text{m}$ . The pore sizes range from 5 to 6 nm. The chitosan film exhibits a smooth surface on the bottom and a rough surface on the upper face (Fig. 3A and B), which is due to only the upper side being in contact with air during the dehydration process. The measurements of the surface arithmetic roughness by AFM (Fig. 4) have shown that the upper face exhibits a mean roughness of  $4.39\text{ nm}$  which is almost five times higher than that of the smooth surface (mean roughness of  $0.901\text{ nm}$ ).

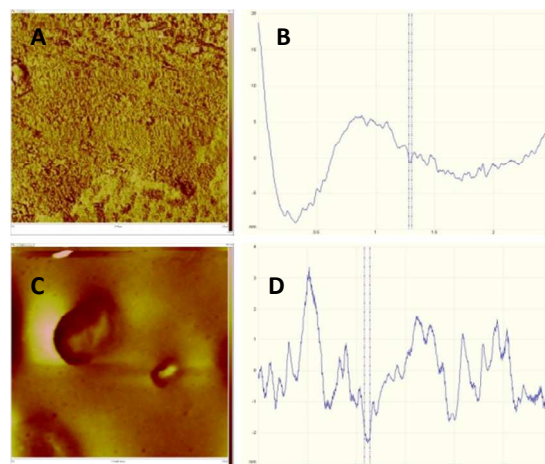


Figure 4: AFM of (A) rough side and (B) smooth side of the dry chitosan film

### 3.2. Characterization of the 3D biocathodes structure

SEM images of the cross-section of the cathode (Fig. 5) show that the chitosan matrix is composed of homogeneous nano-fibres with an average diameter of 30 nm.

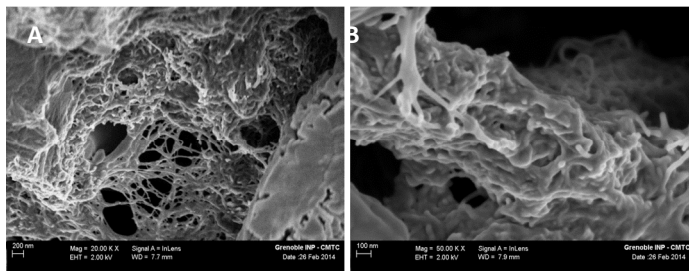


Figure 5: SEM images of a cross-section of Chit-MWCNT-laccase biocathode (A) 20 KX and (B) 50 KX magnifications

We reported a new procedure to obtain conducting polymer nanofibres by simultaneous compression of viscous chitosan, MWCNTs and laccase<sup>12</sup>. The advance in the present work reported here is to use genipin as a crosslinker to enhance the properties of the 3D matrix without changing the nanofibrous structure, which is advantageous for enzyme immobilization and substrates diffusion. In fact, the use of a crosslinker prevents the degradation of chitosan in acidic conditions and after a long period especially *in vivo*. In order to demonstrate that the 3D nanofibrous matrix observed by SEM (Fig. 5) is composed of chitosan and study chemical modifications occurring after implantation, FTIR analysis was performed on biocathodes used as control (stored *in vitro* conditions) and after the two periods of implantation (Fig. 2B). The peaks observed in spectrum (a) are characteristic of chitosan and in accordance with our previous study<sup>12</sup>. Both fingerprint signals of MWCNT and chitosan are present with regards to the intensity of peaks around 3445  $\text{cm}^{-1}$  and 1067  $\text{cm}^{-1}$ . Compared to our previous FTIR analysis of Chit-MWCNT-laccase 3D matrix without genipin cross-linking<sup>12</sup>, in spectrum (a), the peak at 1714  $\text{cm}^{-1}$  corresponding to an aldehyde II (C=O aldehyde stretching) was present while the peak at 1566  $\text{cm}^{-1}$  disappeared. This can be explained by the reaction between the carboxymethyl group of genipin and the amino group of chitosan<sup>22</sup>. A broad peak was noticed at 1262  $\text{cm}^{-1}$  (C-N stretching of amide III). Cross-linking reactions are expected to occur between chitosan, genipin and laccase molecules during the polymerization of chitosan nanofibres. The conjugation of laccase to chitosan<sup>27</sup> and the use of chitosan crosslinked with genipin as immobilization support for laccase<sup>28</sup> and their positive effect on the enzyme stability were reported in literature. The immobilization procedure is different from what we report here. The simultaneous compression of viscous genipin/chitosan with MWCNTs and laccase powder resulted in a nanofibrous 3D arrangement after the solvent (acetic acid) evaporation. Thus, laccase molecules could react with all free amino groups of chitosan, covalently cross-linked with genipin or simply adsorbed on the fibres. Similar peaks as in spectrum (a) were observed but these peaks shifted to 1627  $\text{cm}^{-1}$  and 1242  $\text{cm}^{-1}$  (C-N stretching of amide III) in spectrum (b) and to 1623  $\text{cm}^{-1}$  and 1256  $\text{cm}^{-1}$  in spectrum (c). The similar intensity of the peak at 1627  $\text{cm}^{-1}$  (spectrum (b)) and 1623  $\text{cm}^{-1}$  (spectrum(c)) suggests that no new cross-linking reactions occurred after 167 days *in vivo*. The absorption band in the region 3500-3350  $\text{cm}^{-1}$  corresponds to the amino group of chitosan. The intensity of the absorption band in the region 3500-3350  $\text{cm}^{-1}$  did not decrease in spectra (b) and (c) which indicates that the amino groups of chitosan remained linked to laccase molecules.

### 3.3. *In vitro* electrochemical characterization

We investigated the possible direct electrical connection of laccase to the chitosan conducting nanofibres by Open Circuit Potential (OCP) and cyclic voltammetry measurements.

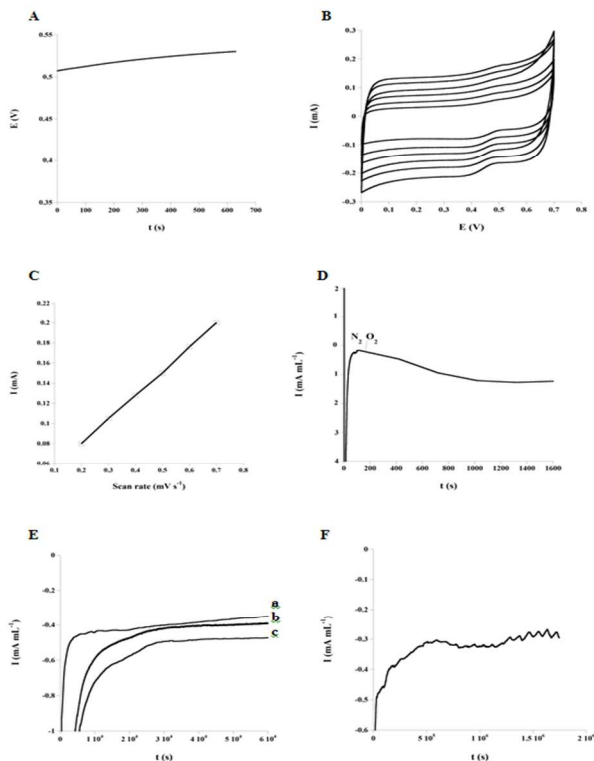


Figure 6: (A) OCP (B) Cyclic voltammetry analysis of the Chit-MWCNT-laccase biocathode at scan rates 0.2, 0.3, 0.4, 0.5, 0.6 and 0.7  $\text{mV s}^{-1}$  (from up to down on the graph), (C) Plot of  $I$  as function of the scan rate, (D) Chronoamperometric response under  $\text{O}_2$  saturation, (E) Comparison of the chronoamperometric responses of the biocathodes under continuous discharge: (a) without genipin cross-linking, (b) electrode based on chitosan cross-linked with genipin and (c) sterilized with gamma radiations, (F) Chit-MWCNT-laccase electrode.

Fig. 6A shows the evolution of the OCP with time for the biocathode. We observe that the OCP increases and tends to stabilize at around 0.53 V vs. SCE which corresponds to the laccase redox potential and in agreement with reported OCP value of laccase directly connected to MWCNTs<sup>10,12</sup>. The cyclic voltammetry (CV) measurements were recorded at low scan rates (from 0.2 to 0.7  $\text{mV s}^{-1}$ ) to subtract the important contribution of capacitive current induced by the large electroactive area of the Chit-MWCNT-laccase network. In Fig. 6B, CV shows the presence of an oxidation peak at 0.52 V and a reduction peak at 0.4 V. The intensities of oxidation peak and reduction peaks increase linearly with the scan rate (Fig. 6C), which indicates that laccase is adsorbed on the surface of electrode, and only the adsorbed laccase are electrically connected to Chit-MWCNT matrix. To check if connected laccase exhibits direct electrocatalytic activity on  $\text{O}_2$  reduction, chronoamperometry measurements were recorded at 0.2 V vs. SCE with and without saturation by  $\text{O}_2$ . Fig. 6D shows that bubbling oxygen into the solution triggers the occurrence of a negative current corresponding to the bioelectrocatalytic reduction of  $\text{O}_2$  that rapidly stabilizes at 1  $\text{mA cm}^{-2}$ , which correspond to 10  $\text{mA mL}^{-1}$  if we consider the

volume of the biocathode. Moreover, the magnitude of this current is two times higher than that obtained in the case of Chit-MWCNT-laccase without using genipin as cross-linker<sup>12</sup>, which indicates that the cross-linking has a positive effect on the biocathode performance.

In order to evaluate the stability of the laccase-based biocathode, chronoamperometry was used to assess the delivered current density. The measured OCP was 0.5 V vs. SCE under continuous discharge, at physiological pH, ambient temperature and without O<sub>2</sub> saturation. As shown in Fig. 6E, the cross-linking of chitosan using genipin (curve (b)) seems to have a positive effect on the current response of the electrode which remained stable as compared to that based on conducting chitosan fibres (curve (a)). The positive effect was accentuated when the electrodes were sterilized by gamma radiations (curve (c)). Although such investigation of the effect of the sterilization procedure is necessary for long-term implantation, few studies reported the effect of gamma radiations on chitosan preparations<sup>29,30</sup>. Khan and co-workers<sup>30</sup> demonstrated that chitosan solutions exposed to low gamma radiation doses (0.1-0.3 kGy) resulted in a positive effect on the mechanical and barrier properties of HEMA grafted chitosan-based films compared to control chitosan films. In our case, chitosan films were polymerized before being exposed to gamma radiations. The used dose (12 kGy) was 40 times higher than the maximal dose described in the study. It was reported that in its film form and exposed to doses from 5 to 100 kGy, the molecular weight of chitosan was not impacted and not subject to radio-degradation<sup>29</sup>. The continuous chronoamperometric measurement showed a stable current response (I around -0.3 mA mL<sup>-1</sup>) during 20 days under continuous discharge (Fig. 6F). This is in accordance with our previous results obtained with Chit-MWCNT-laccase nanofibrous 3D biocathode without crosslinking<sup>12</sup>.

### 3.4. *In vivo* biocompatibility and biodegradability testing

Fig. 7 shows the biocathodes that were recovered after periods of 90 and 167 days *in vivo*. The chitosan film on the surface of the cathodes does not show any visible degradation. A thin tissue membrane has grown on the surface of the cathodes without strong adhesion to the film since it can be easily removed.

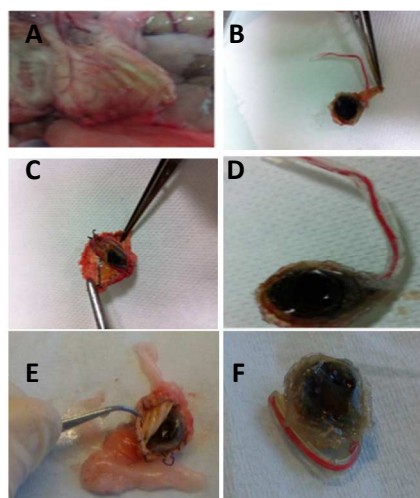


Figure 7: Images of (A) vascularized implant, (B) connective tissue on the cathode, (C) interior of Dacron and (D) film surface after 90 days *in vivo*, (E) interior of Dacron and (F) film surface after 167 days *in vivo*

In order to assess the biocompatibility of the implant, the membrane grown on the surface as well as samples of the tissues and organs surrounding the Dacron were histologically characterized (Fig. 8).

A slight inflammatory reaction occurred in the 14 days after implantation, as indicated by the presence of fat necrosis, fibrin and neutrophils. After 90 days, new tissues and fat layers had grown on the external side of Dacron (Fig. 8C) and a thin layer of mesenchymal tissues had grown on the internal side. After 167 days, the mesenchymal tissue growth was more pronounced on the two sides of Dacron and accompanied by the presence of collagen (Fig. 8E and F). The presence of blood vessels between the tissues indicates that a new vascularized matrix grew around the implant, which is very important for the O<sub>2</sub> supply of the biocathode and also for the glucose supply to a bioanode. As shown in Fig. 8D, the thin tissue membrane which was present on the electrode surface was comprised mainly of a connective tissue.

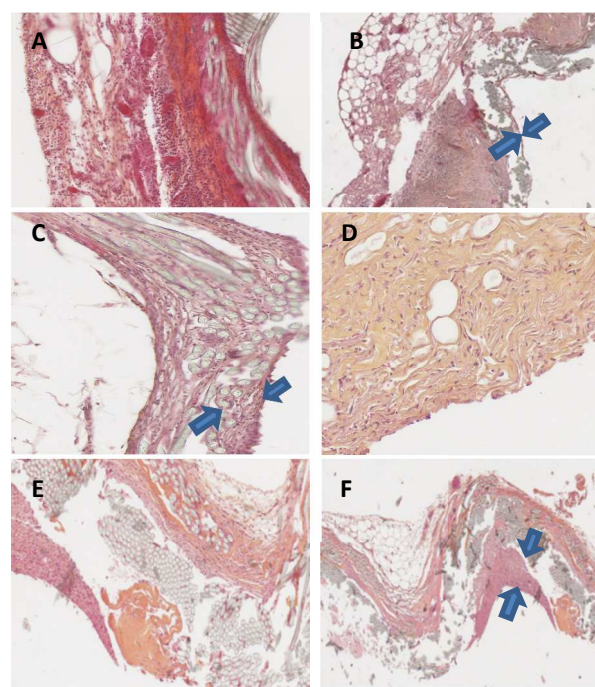


Figure 8: Histological characterization of the implant, (A) and (B) after the period of 14 days, (C) and (D) connective tissue after the period of 90 days, (E) and (F) after the period of 167 days, the blue arrows show the tissue growth at the internal side of Dacron

The absence of inflammatory cells and the growth of new vascularized tissues after 90 and 167 days suggest that the implant was successfully integrated in the rat body. The vascularization is very important to ensure that the surrounding tissues don't form an avascular "scar" which is usually the marker of the formation of a foreign body capsule, a process to encapsulate an implant. Usually, if there is such an absence of blood supply and inhibition of integration, there will be rejection of an implant<sup>31</sup>. In the literature, the biocompatibility of genipin and chitosan has been reported<sup>19</sup>. Kawadkar and Chauhan<sup>32</sup> demonstrated the absence of inflammatory infiltrates after injection of a suspension in saline of genipin cross-

linked chitosan microspheres in the rats' knee. Bavariya and co-workers<sup>33</sup> evaluated the biocompatibility of a chitosan membrane cross-linked with genipin. This membrane exhibits a nanofiber structure and was obtained by electrospinning. The membranes were implanted subcutaneously in the back of rats. They demonstrated the absence of inflammatory cells after 2, 4 and 6 weeks. Their results showed that significant fragmentation of electrospun chitosan membranes did not occur until 20 weeks.

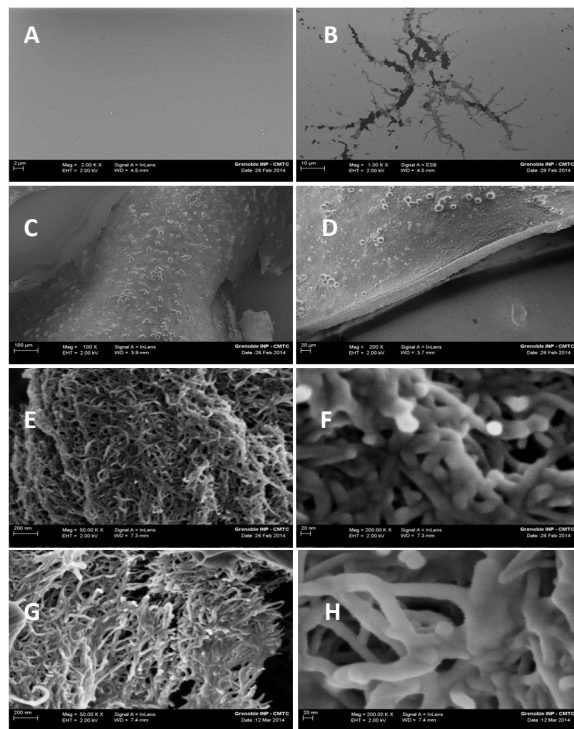


Figure 9: SEM images of (A) and (B) of the chitosan film after 90 days *in vivo*, (C) surface and (D) cross-section of the film after 167 days *in vivo*, the cross-section of the biocathode is illustrated in (E) and (F) after the 90 days, and in (G) and (H) after the period of 167 days

The SEM images of the film structure and the 3D cathode after 90 and 167 days *in vivo* are shown in Fig. 9. Although the formation of a continuous membrane made of connective tissues on the surface of the electrode, the SEM analysis of the chitosan film shows that only few fibroblasts are present (Fig. 9B). The majority of the chitosan film surface is clean which suggests that the connective tissues adhesion was inhibited in the presence of the polymer. This can be confirmed by the absence of new cross-linking reactions with chitosan as we reported above (Fig. 2A). After 167 days *in vivo*, macrophages are present on the surface (Fig. 9B) but not across the chitosan film (Fig. 9C). This demonstrates that the chitosan film formed a successful filtration barrier. The presence of macrophages on the surface may explain the difference between the amide band in spectrum (c) and (d) (Fig. 2A). The role of chitosan in immunostimulation and activation of macrophages has been reported in the literature<sup>32</sup>. The degree of acetylation of chitosan has an effect on the macrophage polarization. In fact, when the deacetylation degree (DA) increases, the percentage of N-acetyl-D-glucosamine units decreases. These units are recognized by the macrophage mannose receptor which is involved in the immune response<sup>35</sup>. In response to chitosan stimulation, macrophages polarize into an anti-inflammatory M2c-like phenotype<sup>34</sup>. Vasconcelos and

collaborators<sup>36</sup> have studied *in vivo* the macrophage response to 3D chitosan scaffolds. They demonstrated that a macrophage M2 reparative response with a lower levels of pro-inflammatory cytokines and higher levels of anti-inflammatory cytokines are induced by a lower DA. In our biocathode, we used highly viscous chitosan that had a degree of DA greater than 80 %. Such a high degree of DA could potentially induce a high amount of M1 pro-inflammatory macrophages due to the immune response in the early stages after implantation. Greater numbers of M1 macrophages are indicative of higher levels of pro-inflammatory cytokines. However, the presence of genipin most likely inhibited this response due to the strong anti-inflammatory effect of genipin. Genipin inhibits the production of nitric oxide (NO), blocks the cyclooxygenase-2 expression and consequently inhibits acute inflammation<sup>37</sup>. In fact, when an inflammatory event takes place, the production of NO increases. This is due to the activity of an inducible nitric oxide synthase (iNOS) which results in cell damages. Cyclooxygenase-2 plays an important role in inflammation since it is involved in the production of prostanoid-like prostaglandins. In a later stage, chitosan stimulates the polarization of anti-inflammatory macrophages. This can explain our observation of macrophages after a longer period of implantation. The fibrous structure of the chitosan matrix doesn't show any degradation after 90 (Fig. 9E) and 167 days (Fig. 9G). The laccase remains adsorbed on the chitosan fibres after both periods (Fig. 9F and H), which confirms the electrical connection of the enzyme and explains the catalytic current that we measured as above. This is further supported by the FTIR results (Fig. 2B) since no significant difference was noticed between spectrum (b) and (c). The absence of new molecules inside the 3D matrix (Fig. 9E and G) and the absence of new cross-linking reactions (spectrum (b) and (c) in Fig. 2B) demonstrates that the observed macrophages were retained by the chitosan film and thus, didn't reached the nanofibres.

### 3.5. *Ex-vivo* electrochemical characterization of the biocathode

In order to check if laccase retains its electrocatalytic activity after implantation, two implanted biocathodes were analyzed. The first one was implanted for 90 days, whereas the second was left for 167 days. For the two cathodes, the OCP at pH 7.4 was between 0.45 V and 0.48 V vs. SCE which is only 20 to 50 mV lower than the biocathode OCP measured before implantation. Fig. 10A and B show the chronoamperometry responses of the two biocathodes at pH 7.4 and without oxygen saturation.

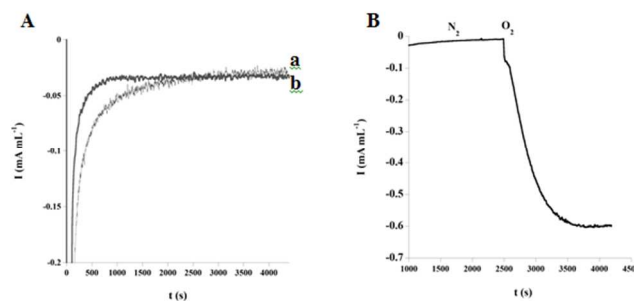


Figure 10: (A) Chronoamperometric response of the Chit-MWCNTs-laccase biocathode under air conditions and pH 7.4, (a) after 90 days *in vivo*, (b) after 167 days *in vivo*, (B) Chronoamperometric response of the Chit-MWCNT-laccase biocathode under oxygen saturation

The measured current density is around  $-0.03 \text{ mA mL}^{-1}$  (Fig. 10A), which represents about 7.5 % of the measured current *in vitro* at pH

7.4. Nonetheless, these results don't allow a complete estimation of the remaining electroactive laccase available in the bioelectrode. In fact, it is possible that inside the polymer matrix, more laccase molecules remain active since the pH is different from the physiological pH of the biocathode environment. Thus, it is likely that the internal pH is more acidic, since the measured output of the enzyme was quite stable. In order to estimate the remaining laccase activity inside the biocathode, we analyzed the current output in solution near the optimum pH of laccase (pH 5) with and without O<sub>2</sub> saturation (Fig. 10B). Indeed, the chronoamperometric response of the bio-cathode implanted during 167 days was recorded at 0.2 V vs. SCE with and without O<sub>2</sub>. Fig. 10B shows the appearance of a cathodic current ( $-0.6 \text{ mA mL}^{-1}$ ) after O<sub>2</sub> saturation. This response to oxygen saturation corresponds to the catalytic reduction of dioxygen by laccase. These results indicate the continued presence of immobilized enzymes which retained activity after 167 days of implantation. The measured catalytic current density is 50 % lower than that measured before implantation under oxygen saturation (Fig. 6D). Unlike the results obtained at pH 7.4, these results show that the biocathode preserves half of its electro catalytic activity after more than five months of implantation.

From these results, we believe that the large loss of the electrocatalytic activity of the biocathode at pH 7.4 is not related to inhibition or disconnection of the majority of laccase present in the biocathode. Indeed, if laccase molecules were inhibited or disconnected we would not have observed their catalytic activity at pH 5. Consequently, the large decrease of the performance of the biocathode at physiological pH can be attributed to a modification of the microenvironment around the laccase inside the biocathode. Although a MWCNTs-laccase biocathode was not stable for more than one month during *in vitro* conditions<sup>10</sup>, the Chit-MWCNT matrix that we prepared and reported here was able to protect the laccase during the implantation period. These results are very important for the development of an implantable glucose biofuel cell able to operate for a long period and to the best of our knowledge, we report the first study of an implantable biocathode lifetime.

#### 4. Conclusions

We demonstrate that the use of a Chit-MWCNT matrix, fabricated by mechanical compression, allows construction of a biocompatible enzymatic biocathode which remains operational after more than five months implanted *in vivo* (retaining 50 % of its initial electrocatalytic activity). To the best of our knowledge, this is the best performance obtained with an implanted enzymatic bioelectrode for a long period *in vivo* implanted in a freely moving animal. For comparison, the previous longest duration of performance *in vivo* was for a biocathode implanted in a snail for two weeks (Table 1).

Table 1. Comparison of the lifetime reported for different implanted biocathodes

Animal/location	Catalyst used in the biocathode	Operational lifetime	Reference
Rat/retroperitoneal space	Polyphenol oxidase	11 days	1
Rat/retroperitoneal space	Laccase	9 days	2
Rat/brain	Bilirubin oxidase	Several hours	6
Clams/ dorso-posterior part	Laccase	Lower than a week	5
Snail/ between the body wall and internal organs	Laccase	2 weeks	38
Rat/ jugular vein	Platinum	24 hours	3

Also, MacVittie and coworkers<sup>5</sup> demonstrated, when implanted in other animals than mammals, that a GBFC with laccase-based biocathode was operational few days inside clams and two weeks inside a snail. No previous reports describe *ex vivo* measurements the current response of the bioelectrodes after implantation and particularly which bioelectrode is responsible for the degradation of the output an implanted GBFC.

In our previous work<sup>2</sup>, we demonstrated that an implantable GBFC using laccase at the biocathode was operational for 9 days inside a rat. The short lifetime of that GBFC was attributed to the loss electrical connection of the GBFC which precluded any subsequent *ex vivo* measurements. In this study, we focussed on the biocathode since its limited stability over time usually affects the overall stability of the GBFC. The stability of the bioelectrode *in vivo* may vary depending if a continuous or a discontinuous discharge is applied, but those measurements require an implanted device that can report in real-time the performance of the implanted biocathode during a long period.

We report the longest *in vivo* duration for a Chit-MWCNT-laccase biocathode to maintain stable electrical output (almost 6 months). The enhanced longevity is due to a new design that resists degradation of the biocathode by the body fluids and improves the biocompatibility. Furthermore, the 3D matrix of nanofibrous chitosan crosslinked with genipin provided an efficient protective environment for laccase molecules since they retained their electrocatalytic activity in subsequent bench-top measurements after removal of the biocathode at the end of the implantation period. The new strategy reported in the present study ensured both the operational stability over time and also the *in vivo* biocompatibility of the bioelectrode. The results we report here are important for the electrochemical and biomedical communities, since they constitute the first demonstration of the biocompatibility in addition to the role of the bioelectrode design in preventing enzyme activity loss inside the body. This implantation strategy is now being tested for a biofuel cell.

#### Acknowledgements

We thank the ANR (MGBFC-EMMA-043, 2011-2013) and the Investissements d'Avenir (ANR-10-NANO-03-01, 2012-2016) for financial support. We thank Frédéric Charlot (CMTC, Grenoble) for producing the SEM images and Cécile Bruzzese Sillard (Grenoble INP-Pagora) for producing the AFM images. We thank Laurent Cortella (CEA, Grenoble) for the gamma sterilization experiments and the Laboratoire des Radiopharmaceutiques Biocliniques (LRB), especially to Audrey Soubies for care, handling and establishing an enriching environment for the rats.

#### Notes and references

<sup>a</sup> Univ. Grenoble 1 – Joseph Fourier / CNRS / INSERM / TIMC-IMAG UMR 5525, Grenoble, F-38041, France. E-mail: don.martin@imag.fr

<sup>b</sup> University of Grenoble Alpes / CNRS / LGP2 UMR 5518, F-38000, France

<sup>c</sup> Laboratory of Cytology, Biochemistry and Cytopathology, Centre Hospitalo-Universitaire Albert Michallon, B.P. 217X Cédex 9, 38043 La Tronche Cedex, France

1 P. Cinquin, C. Gondran, F. Giroud, S. Mazabrard, A. Pellissier, F. Boucher, J.-P. Alcaraz, K. Gorgy, F. Lenouvel, S. Mathé, P. Porcu and S. Cosnier, *PLoS ONE*, 2010, **5** (5), e10476.

- 2 A. Zebda, S. Cosnier, J.-P. Alcaraz, M. Holzinger, A. Le Goff, C. Gondran, F. Boucher, F. Giroud, K. Gorgy, H. Lamraoui, P. Cinquin, *Sci. Rep.* 2013, **3**, 1516.
- 3 F.C.P.F. Sales, R.M. Iost, M.V.A. Martins, M.C. Almeida and F.N. Crespihlo, *Lab Chip* 2013, **13**, 468.
- 4 J.A. Castorena-Gonzalez, C. Foote, K. MacVittie, J. Halánek, L. Halámková, L.A. Martínez-Lemus and E. Katz, *Electroanal.* 2013, **25(7)**, 1579.
- 5 K. MacVittie, J. Halánek, L. Halámková, M. Southcott, W.D. Jemison, R. Lobel and E. Katz, *Energy Environ. Sci.* 2013, **6**, 81.
- 6 V. Andoralov, M. Falk, D.B. Suyatin, M. Granmo, J. Sotres, R. Ludwig, V.O. Popov, J. Schouenborg, Z. Blum and S. Shleev, *Sci. Rep.* 2013, **3**, 3270.
- 7 E. Katz and K. MacVittie, *Energy Environ. Sci.* 2013, **6**, 2791.
- 8 S. Cosnier, A. Le Goff and M. Holzinger, *Electrochem. Commun.* 2014, **38**, 19.
- 9 H. Shin, C. Kang and A. Heller, *Electroanal.* 2007, **19(6)**, 638.
- 10 F. Xu, *Biochemistry* 1996, **35**, 7608.
- 11 C. Vaz-Dominguez, S. Campuzano, O. Rüdiger, M. Pita, M. Gorbacheva, S. Shleev, V.M. Fernandez and A.L. De Lacey, *Biosens. Bioelectron.* 2008, **24(1)**, 531.
- 12 A., Zebda, C. Gondran, A. Le Goff, M. Holzinger, P. Cinquin and S. Cosnier, *Nature Commun.* 2011, **2**, 370.
- 13 B. Reuillard, A. Le Goff, C. Agnès, M. Holzinger, A. Zebda, C. Gondran, K. Elouarzaki and S. Cosnier, *Phys. Chem. Chem. Phys.* 2013, **15**, 4892.
- 14 S. El Ichi, A. Zebda, A. Laaroussi, N. Reverdy-Bruas, D. Chaussy, M.N. Belgacem, P. Cinquin and D.K. Martin, *Chem. Commun.* 2014, **50**, 14535.
- 15 M. Rinaudo, *Prog. Polym. Sci.* 2006, **31**, 603.
- 16 C. Peniche, W. Argüelles-Monal and F.M. Goycoolea, in *Monomers, Polymers and Composites from Renewable Resources*, Elsevier B.V. Ed., 2008, pp. 517–542.
- 17 F. Croisier and C. Jérôme, *European Polym. J.* 2013, **49**, 780.
- 18 T. Jiang, R. James, S.G. Kumbar and C.T. Laurencin, in *Natural and Synthetic Biomedical Polymers*, Elsevier Inc. Ed. 2014, pp. 91–113.
- 19 R. Jayakumar, D. Menon, K. Manzoor, S.V. Nair and H. Tamur, *Carbohydr. Polym.* 2010, **82**, 227.
- 20 B. Krajewska, *Enz. Microb. Technol.* 2004, **35**, 126.
- 21 J. Jin, M. Song and D.J. Hourston, *Biomacromol.* 2004, **5**, 162.
- 22 R.A.A. Muzzarelli, *Carbohydr. Polym.* 2009, **77**, 1–9.
- 23 M.F. Butler, Y.F. Ng and P.D.A. Pudney, *J. Polym. Sci. Part A: Polym. Chem.* 2003, **41**, 3941.
- 24 K.Yao, J. Li, F. Yao and Y. Yin, in *Chitosan based hydrogels – Functions and applications*, Taylor & Francis Group, LLC Ed. 2011.
- 25 J. Kumińska, M. Czerwicka, Z. Kaczyński, A. Bychowska, K. Brzozowski, J. Thöming and P. Stepnowski, *Marine Drugs* 2010, **8**, 1567.
- 26 S. Kumar, J. Koh, H. Kim, M.K. Gupta and P.K. Dutta, *Int. J. Biol. Macromol.* 2012, **50**, 493.
- 27 E. Mirzaei, R. Faridi-Majidi, M.A. Shokrgozar and F.A. Paskiabi, *Nanomed. J.* 2014, **1(3)**, 137.
- 28 Y. Dong, C. Xu, J. Wang, M. Wang, Y. Wu and Y. Ruan, *Science in China (Series B)* 2001, **44**, 216.
- 29 G. Delanoy, Q. Li and J. Yu, *Intern. J. Biol. Macromol.* 2005, **35**, 89.
- 30 S.C. Fernandes, D.M.P.O. Santos and I.C. Vieira, *Electroanalysis* 2013, **25(2)**, 557.
- 31 C. Vanichvattanadecha, P. Supaphol, N. Nagasawa, M. Tamada, S. Tokura, T. Furuike, H. Tamura and R. Rujiravanit, *Polymer Degradation and Stability* 2010, **95**, 234.
- 32 A. Khan, T. Huq, R.A. Khan, D. Dussault, S. Salmieri and M. Lacroix, *Radiation Phys. Chem.* 2012, **81**, 941.
- 33 E.M. Sussman, M.C. Halpin, J. Muster, R.T. Moon and B.D. Ratner, *Ann. Biomed. Eng.* 2014, **42(7)**, 1508.
- 34 J. Kawadkar and M.K. Chauhan, *European J. Pharma. Biopharma.* 2012, **81**, 563.
- 35 A.J. Bavariya, P.A. Norowski, K.M. Anderson, P.C. Adatrow, F. Garcia-Godoy, S.H. Stein and J.D. Bumgardner, *J. Biomed. Mater. Res. Part B* 2014, **102B**, 1084.
- 36 M.I. Oliveira, S.G. Santos, M.J. Oliveira, A.L. Torres and M.A. Barbosa, *European Cells and Materials* 2012, **24**, 136.
- 37 Z. Xia, and J.T. Triffitt, *Biomed. Mater.* 2006, **1(1)**, R1.
- 38 D.P. Vasconcelos, A.C. Fonseca, M. Costa, I.F. Amaral, M.A. Barbosa, A.P. Águas and J.N. Barbosa, *Biomater.* 2013, **34**, 9952.
- 39 H.-J. Koo, K.-H. Lim, H.-J. Jung and E.-H. Park, *J. Ethnopharmacol.* 2006, **103**, 496.
- 40 L. Halamkova, J. Halamek, V. Bocharova, A. Szczupak, L. Alfonta and E. Katz, *J. Am. Chem. Soc.* 2012, **134(11)**, 5040.

We demonstrate that the use of Chit-MWCNT matrix, fabricated by mechanical compression, allows construction of a biocompatible enzymatic biocathode which remains operational after more than five months *in vivo* (retaining 50 % of its initial electrocatalytic activity)

